ELECTROMAGNETIC TORQUE ESTIMATION OF A THREE-PHASE INDUCTION MOTOR FOR SETTING THE FEEDRATE OF A MILLING MACHINE

Élida Fernanda Xavier Júlio
Postgraduation Program in Mechanical Engineering, Federal University of Paraíba, Cidade Universitária, CEP 58059-900, João Pessoa, PB, Brazil.
elida_xnet@yahoo.com.br

Simplício Arnaud da Silva[1]
Isaac Soares de Freitas[2]
Cícero da Rocha Souto[3]
Lucas Vinicius Hartmann[4]
Department of Electrical Engineering, Federal University of Paraíba, Cidade Universitária, CEP 58059-900, João Pessoa, PB, Brazil.
[1] sarnaud@cear.ufpb.br
[2] isaacfreitas@cear.ufpb.br
[3] cicerosouto@cear.ufpb.br
[4] lucas.hartmann@cear.ufpb.br

Abstract. *In this paper, it is presented a project of a fuzzy controller and a neural estimator to control a coordinate table powered by three-phase induction motor, aiming to implement an intelligent milling system. The position/speed control is performed using vector techniques of three-phase induction machines. The estimation of the motor electromagnetic torque is used for setting the feedrate of the table. The speed control is developed using Takagi-Sugeno fuzzy logic model and electromagnetic torque estimation using neural network type LMS algorithm. The induction motor is powered by a frequency inverter driven by a Digital Signal Processor (DSP). Control strategies are implemented in DSP. Simulation results are presented for evaluating the performance of the system.*

Keywords: machining, speed control, torque estimation, fuzzy logic, neural network.

1. INTRODUCTION

Milling is a machining process in which the piece material removal takes place intermittently. The milling is accomplished by the combination of two movements performed simultaneously. One of the movements is rotation of the cutter around its axis. The other is the movement of the milling machine table, which is attached to the piece to be milled. Thus, cutting parameters such as feedrate, cutting speed and cutting depth should be analyzed (Alves, 2002). According to Mao-Yue *et al.* (2009), parameters of the machining process should be monitored and adjusted automatically, which can improve the production quality and reduce the machining time.

With advancements in applications using induction motors, the use of these motors on start and controlling of positioning systems are majority in the industry. An example of positioner machine is the coordinate table, which has applicability to devices milling, turning, drilling, and welding, among others. The milling operation is one of the most important in the process of mechanical machining.

The three-phase induction motor is widely used in various applications in industry, due to its relative simplicity of construction, maintenance, both operational and market low cost, as well as, the capacity to operate with a wide range of loads in adverse conditions. One of the factors that provided the advancement in driving of three-phase induction motor was the development of control strategies, specifically vector control strategies.

In induction machine, the implementation of vector control for field orientation can be done by direct or indirect method. The direct field orientation enables the position of the flux is determined by measuring terminal quantities of the stator (voltages and currents). The advantage of using the stator terminal quantities lies in the fact to be sensitive only to the stator resistance (Altuna, 1997).

In the development of controllers and estimators, and the use of vector control, the application of intelligent control techniques, such as fuzzy logic and artificial neural network (ANN), provided greater robustness to systems powered by three-phase induction motors.

Fuzzy logic is a technique that allows the implementation of human experience in systems, considering the uncertainty of information, the ambiguities, for the development of controllers. The fuzzy inference model type Takagi-Sugeno (TS) is capable of representing, approximately or exactly, any nonlinear dynamics as combination of locally valid linear models, interpolating smoothly (Mozelli, 2008). The TS fuzzy model is a hybrid approach (Takagi and Sugeno, 1985), because it combines a fuzzy method based on rules and a mathematical method, consisting of

conditional propositions, whose antecedents are linguistic variables and whose consequents are linear equations (Shaw and Simões, 2004).

The ANN is a computational technique organized according on human neural structures and acquires knowledge from experience, consisting of inherently parallel and adaptive processing (Nigrini, 1993). This technology has the proper way to store knowledges and to evaluate them for use (Rumelhart and Mcclelland, 1986). This knowledge is acquired through a learning process and stored in a distributed manner. The learning objective is to obtain an implicit model of the system under study by adjusting the parameters of the neural network (Leite, 2003).

In machining systems, a structure consisting of artificial neural network and data set was applied in the work by Lin *et al.* (2006), in order to obtain the inference of knowledge of a fuzzy model for an end milling process. The inference, based on fuzzy learning, was used as a mechanism of intelligent determination of advancement.

The signal digital processor is a device that performs signal acquisition, performs large number of mathematical operations with fast and efficient processing in the range of microseconds, enabling the application in high performance systems operating in real time (Severino, 2005). This equipment is well suited for the implementation of control and estimation strategies, which have complex calculations to be performed in real time.

This paper presents simulated results for the development of a driving and control system of a vertical milling machine. This system drives the coordinate table of the milling machine with specific feedrate for machining of material of a piece.

As the coordinate table is driven by three-phase induction motor, the angular position control and the rotor rotational speed control of this motor are carried out. This speed of the three-phase induction motor is controlled using Takagi-Sugeno fuzzy control system.

The electromagnetic torque of the motor is estimated in order to identify the material of the machined piece and to define the feedrate of the table. For this estimation, it is used an artificial neural network type LMS (Least Mean Square) algorithm.

2. SYSTEM DEVELOPMENT

For the experimental setup of the milling machine, design shown in Fig. 1, it will be used a X-Y coordinate table composed by two perpendicular bases to each other, X and Y, which move linearly in the horizontal plane. The X base of the table (upper base) has a course of 200 mm and the Y base (lower base) of 100 mm, whose trapezoidal spindles have a pitch of 4 mm for ten revolutions of the motor shaft. Each base of the table is driven by a three-phase induction motor. The drive of the X base results in displacements in the right and left directions, and the Y base results in forward and backward displacements.

A tool of end mill will be attached on the mandrel, located in the spindle of the milling machine. The cutter, running through a cutting depth in the Z axis, will perform chip removal of a piece fixed to the X base.
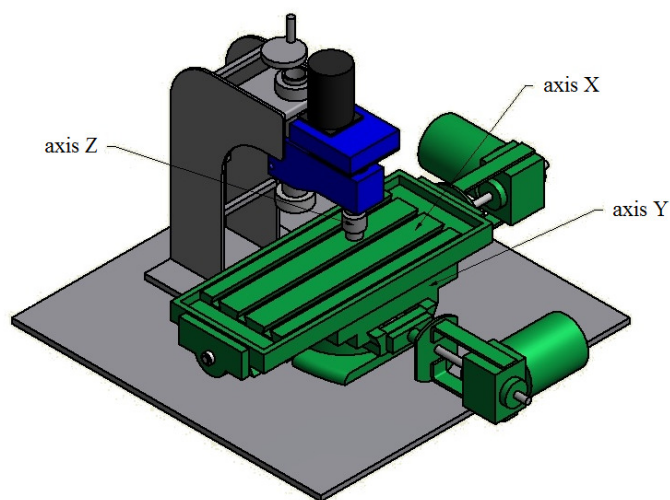

Figure 1. Vertical milling machine design.

Due to the work of piece machining, an electromagnetic torque will be imposed on the induction motor of the X base. The information of the electromagnetic torque estimated will characterize the type of material constituent of the piece. This signal of the estimated torque will be used to specify, in real time, the drive speed of the X base.

In Figure 2, the system configuration for the drive and control of the X base of the coordinate table is schematized. In this diagram, it can be observed not only the control system, developed to drive and control the three-phase induction motor of the X base, but also the estimation system of the electromagnetic torque of this motor.

A DSP is used for processing, transmission and data acquisition. Hardware consists of a three-phase voltage inverter will power the three-phase induction motor of the table. An encoder is coupled to the motor shaft in order to obtain the angular position of the rotor of this machine and thus the linear position of the X base. And sensors are used to obtain the phase currents and phase voltages of the motor.
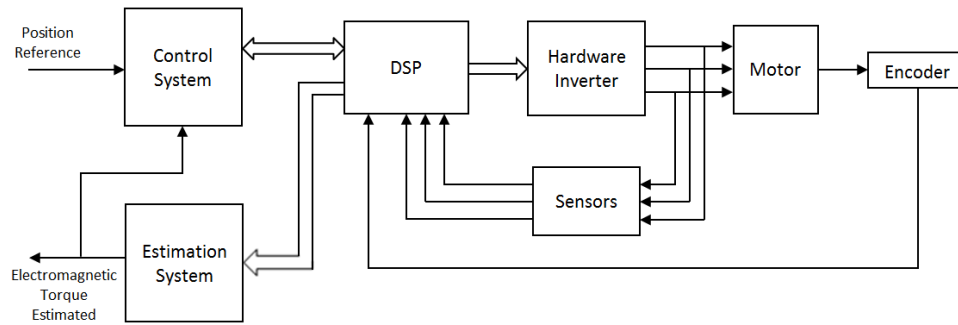
Figure 2. Schematic diagram for the control of the coordinate table.

2.1 Control system

The control system of the three-phase induction motor was implemented in closed loop, where it was developed: a current controller using a proportional-integral controller (PI), and a speed controller through fuzzy model TS.

The speed controller is composed: of a fuzzy PD base, TS model, with an input of Error and another Derror; and the integration of the Error. In Figure 3, it is presented the structure of the PD+I speed fuzzy controller used, in which i_{ts} is the output variable of the fuzzy PD base, k_p is the gain and i_{sq}^{b*} is the control variable. The variable i_{sq}^{b*} corresponds to the stator current of the three-phase induction motor, q component in referential of the rotor flux.
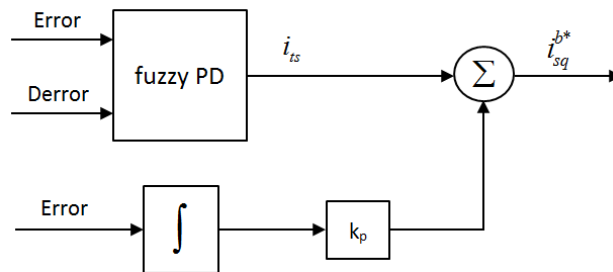
Figure 3. PD+I speed fuzzy controller.

Next, the settings for fuzzification, fuzzy inference and defuzzification of the developed fuzzy PD base are presented.

In the fuzzification stage, Error and Derror input variables are defined, respectively, by the difference between the reference value and the value of the rotor rotational speed ω_r, and by the derivative of this error. The universes of discourse of the Error and Derror comprise a normalized range from -1 to 1.

The variable Error is composed of seven pertinence functions, with triangular and trapezoidal shapes, called: NB (Negative Big), NM (Negative Medium), NS (Negative Small), AZ (Almost Zero), PS (Positive Small), PM (Positive Medium) and PB (Positive Big). In Figure 4, it is presented the arrangement of linguistic terms of the Error in their universe of discourse.

For variable Derror, it was associated seven pertinence functions, with triangular and trapezoidal shapes, defined by the terms: NB, NM, NS, AZ, PS, PM and PB. In Figure 5, these functions are shown.

In the stage of fuzzy inference, it is determined how the control rules are activated. In Table 1, the forty-nine control rules developed are inserted.

Control rules consist of conditional sentences. For the composition of each rule and for the relationship between them, the *max-min* inference technique was used. Thus, each sentence is modeled by the *min* application and the relationships between rules are modeled by the *max* application.
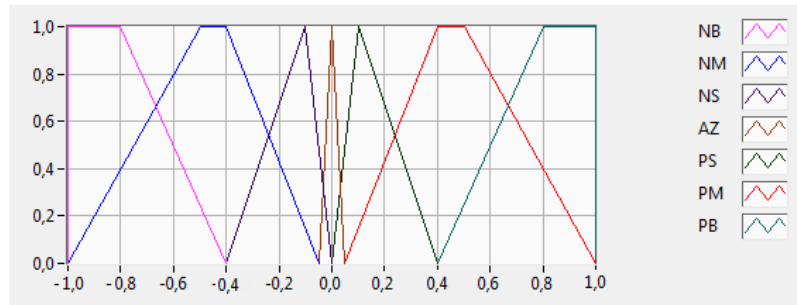
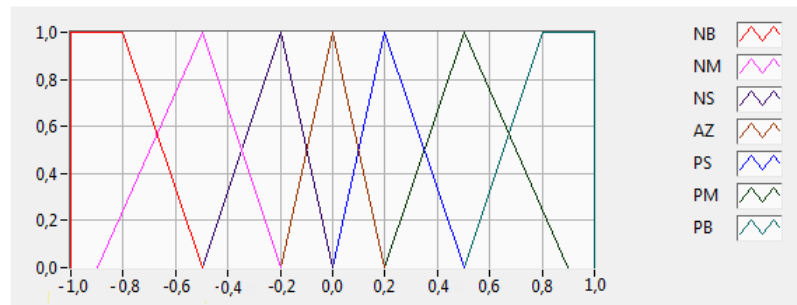Figure 4. Pertinence functions of the Error input variable.

Figure 5. Pertinence functions of the Derror input variable.

Table 1. Table of fuzzy rules of the speed controller.

Error \ Derror	NB	NM	NS	AZ	PS	PM	PB
NB	iNB	iNB	iNB	iNB	iPM	iPB	iPB
NM	iNB	iNB	iNB	iNM	iPS	iAZ	iPB
NS	iNB	iNB	iNM	iNS	iAZ	iPS	iPM
AZ	iPB	iPM	iPS	iAZ	iNS	iNM	iNB
PS	iNM	iNS	iAZ	iPS	iPM	iPB	iPB
PM	iNB	iAZ	iNS	iPM	iPB	iPB	iPB
PB	iNB	iNB	iNM	iPB	iPB	iPB	iPB

In the defuzzification, the i_{ts} output variable is generated, according to the PD fuzzy output shown in Fig. 3. According to Takagi-Sugeno fuzzy method, at this stage, a linear and time-invariant model is determined (Milhor, 2008).

In Equation (1), i_{ts} variable is obtained by a weighted average, in which the i_{tsx}, i_{tsy} and i_{tsz} terms are expressed by Eq. (2), Eq. (3) and Eq. (4), respectively. This equation consists of linear functions, defined from the consequents of control rules and the numerical values of the Error and Derror input variables.

$$i_{ts} = \frac{i_{tsx} + i_{tsy} + i_{tsz}}{iNB + iNM + iNS + iAZ + iPB + iPM + iPS} \tag{1}$$

$$i_{tsx} = iNB(30 \cdot Error - 0,1 \cdot Derror) + iNM(70 \cdot Error - 0,3 \cdot Derror) + iNS(90 \cdot Error - 0,5 \cdot Derror) \tag{2}$$

$$i_{tsy} = iAZ(1,0 \cdot Error - 1,0 \cdot Derror) \tag{3}$$

$$i_{tsz} = iPB(30 \cdot Error - 0,1 \cdot Derror) + iPM(70 \cdot Error - 0,3 \cdot Derror) + iPS(90 \cdot Error - 0,5 \cdot Derror) \tag{4}$$

The project of the current controller was developed from the complex model of representation of a three-phase induction machine, using the control quadrature with referential in rotor flux (*b*).

Through the realization of mathematical simplifications, it was obtained the transfer function used in the project of current controller, as Eq. (5), where I_s^b and $V_s^{b'}$ correspond to the stator current and stator voltage of the three-phase induction motor in the referential of the rotor flux, respectively. Equations (6) and (7) are constituted by the parameters of the three-phase induction motor, in which l_s is the cyclic stator inductance, l_r is the cyclic rotor inductance, l_m is the cyclic mutual inductance, R_s is the stator resistance and τ_r is the rotor time constant.

$$I_s^b = \frac{l_r\sigma}{(s+\eta)}V_s^{b'} \tag{5}$$

$$\sigma = \frac{1}{l_s l_r - l_m^2} \tag{6}$$

$$\eta = l_r\sigma R_s + \frac{\sigma l_m^2}{\tau_r} \tag{7}$$

For the development of the current controller was used a PI classical controller, whose gains k_{p_i} and k_{i_i} were determined by Eq. (8) and (9), respectively. In Equation (8), T_v is the time constant of the source.

$$k_{p_i} = \frac{1}{4T_v l_r\sigma} \tag{8}$$

$$k_{i_i} = \eta \cdot k_{p_i} \tag{9}$$

2.2 Estimation system

From the complex model of representation of three-phase induction machine developed the estimation project of the electromagnetic torque of the three-phase induction motor, using control quadrature with fixed reference in the stator (*a*) and applying a ANN type LMS algorithm.

An equation widely used to estimate the electromagnetic torque is Eq. (10), which is written in terms of the components of the stator flux and stator current. Thus, for the estimation of electromagnetic torque, firstly, stator flux of the three-phase induction motor was estimated.

$$ce = P\left(i_{sq}^a \lambda_{sd}^a - i_{sd}^a \lambda_{sq}^a\right) \tag{10}$$

In applying the voltage model of the machine, in the direct field orientation with reference by stator flux, the estimate stator flux $\boldsymbol{\lambda}_s^a$ is obtained by integrating the counter-electromotive force. Equations (11) and (12) correspond to the stator flux in the *d* and *q* components, respectively. The stator voltage $\mathbf{v}_s^a$ and stator current $\mathbf{i}_s^a$ variables were obtained from the motor terminals. The stator resistance R_s is considered constant and equal to 5.1 Ω.

$$\lambda_{sd}^a = \int\left(v_{sd}^a - R_s i_{sd}^a\right)dt \tag{11}$$

$$\lambda_{sq}^a = \int\left(v_{sq}^a - R_s i_{sq}^a\right)dt \tag{12}$$

The integration procedure of counter-electromotive force originates levels of continuous current, called *offset*, in the estimation of the stator flux, implying, therefore, on an estimation of electromagnetic torque with not tolerable errors.

For eliminating the *offset* on the flux signal, a neural adaptive filter was developed by the LMS algorithm technique. A neural structure was implemented for each flux component, *d* and *q*, similarly.

In Figure 6, this structure is presented for the *d* component, consisting of only one neuron and a *bias*, as synaptic weight, with constant input equal to 1. The neural structure has, as input, the signal from the estimated stator flux λ_{sd}^a and the filtrated estimated stator flux λ_{sdf}^a is obtained in the output. The filtering process is performed by subtracting "*y*" of the input signal λ_{sd}^a.

The algorithm developed for representation of the neural structure is described in Eq. (13) and Eq. (14), where $y(n)$ is the filter output at the current instant and $y(n+1)$ is the filter output at the next instant. Through this algorithm, an adaptive iteration was effected to each acquisition of the input data.

$$\lambda_{sdf}^a = \lambda_{sd}^a - y(n) \tag{13}$$

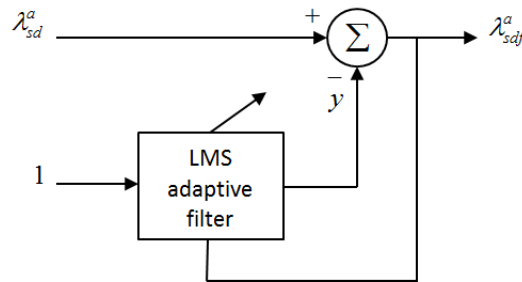$$y(n+1) = y(n) + 2\mu\lambda_{sdf}^a \tag{14}$$

Figure 6. Neural structure with LMS adaptive filter.

The learning rate μ, used in Eq. (14), was calculated by the Eq. (15), so that μ is obtained in function of speed ω_r because specific learning rates, due to variation of speed ω_r, were required.

$$\mu = -3,5625 \cdot 10^{-7} \cdot \omega_r + 2,4884375 \cdot 10^{-4} \tag{15}$$

After the estimation of the stator flux and the elimination of the *offset* in the flux signal, the electromagnetic torque of the motor was estimated using Eq. (16). In this equation, the estimated electromagnetic torque ce_{est} is determined using the filtered estimated stator flux, λ_{sdf}^a and λ_{sqf}^a the stator current, i_{sd}^a and i_{sq}^a, and the constant of the number of pairs of poles P of the three-phase induction motor, which is equal to two.

$$ce_{est} = P\left(i_{sq}^a \lambda_{sdf}^a - i_{sd}^a \lambda_{sqf}^a\right) \tag{16}$$

3. SIMULATION RESULTS

In milling system, the objective is to drive the X base of the table for machining pieces constituted by different materials. To perform this study, in the simulation of the operation of the three-phase induction motor, the application of various loads to the motor was simulated and information of the torque signal ce_{est} was used in the specification of the speed reference of rotation of the rotor ω_r^* for the motor drive.

The milling machine table performs a displacement of 4 mm for every ten revolutions of the motor shaft. Therefore, it was determined a numerical factor of the relationship between the magnitudes of linear displacement and linear speed of the table and the magnitudes of angular displacement and angular speed of the three-phase induction motor, that is 0.064 mm/rad.

In Table 2, the values, in module, are shown: the electromagnetic torques ce and their speed references ω_r^*, and, through the ratio factor, the equivalent speed references of the X base v*.

For analysis of the response curves, the induction motor is driven by references the type of step position, with amplitudes of 1562.5 rad and -1562.5 rad, resulting in rotation of the motor shaft in clockwise and anticlockwise directions. The aim is to analyze the displacement of the X base in right and left directions, along its 200 mm course.

Table 2. Electromagnetic torques and reference speeds (values in module).

ce (N.m)	ω_r^* (rad/s)	v^* (mm/s)
1.0	31.0	1.984
2.0	27.0	1.728
3.0	23.0	1.472
4.0	19.0	1.216
5.0	15.0	0.96

The simulated three-phase induction motor has the following parameters: R_s = 5.1 Ω, R_r = 4.4578 Ω, $l_s = l_r$ = 0.334 H, l_m = 0.3185 H, F = 0.0041 Nms, J = 0.041 kgm^2. The simulation was performed in C language using the C++Builder® XE computer program and response curves were plotted using the Matlab^{TM} program.

3.1 First simulation

Initially, in Fig. 7, the response and reference curves of the variable angular position of the rotor are presented. In this first simulation, the induction motor was driven with a step type reference signal with amplitude of 1562.5 rad, applying a load of 1 N.m from starting of the machine and, after 30 s of operation, a load of 3 N.m was applied. Due to load applications, electromagnetic torques were imposed to the three-phase induction motor.

In Figure 8, the response and reference curves of the variable position of the X base are shown, in which the step reference signal with amplitude of 100 mm is equivalent to a step of 1562.5 rad. This amplitude of linear magnitude corresponds to a displacement of the X base of the table to position 100 mm. Through the graphics of Fig. 7 and Fig. 8, it was possible to verify a settling time of 57.72 s, a steady state error of 0.13 % and non-occurrence of overshoot.

Then, in Fig. 9, the reference curve of rotational speed of the rotor and the response curve obtained are presented. In this curve, it can be observed the three-phase induction motor drive by a ramp signal speed with amplitude of 31 rad/s, in the upward direction, keeping constant speed until the instant of 30 s. This constant speed of 31 rad/s corresponds to the ω_r^* excitation due to an estimation of electromagnetic torque of 1 N.m, according to Tab. 2. At the instant 30 s, due to the estimation of electromagnetic torque of 3 N.m, a speed ramp with an amplitude of 23 rad/s was observed in the downward direction, remaining constant up to a drive ω_r^* at null value, resulting, thus, in the braking of the three-phase induction motor.
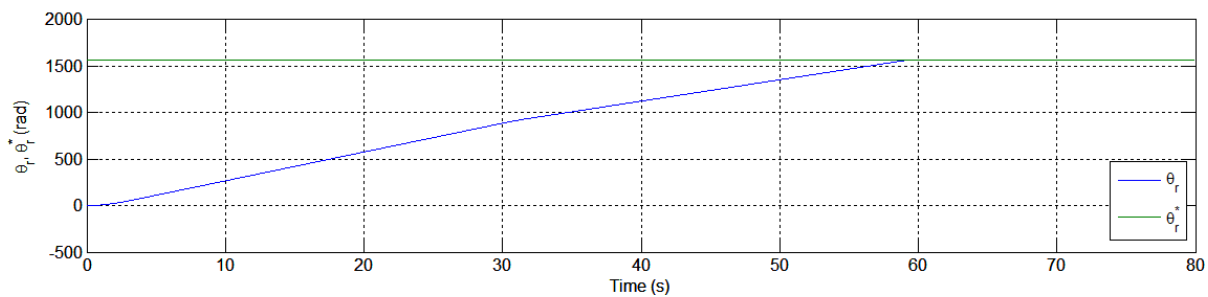

Figure 7. Response and reference curves of the angular position of the rotor.
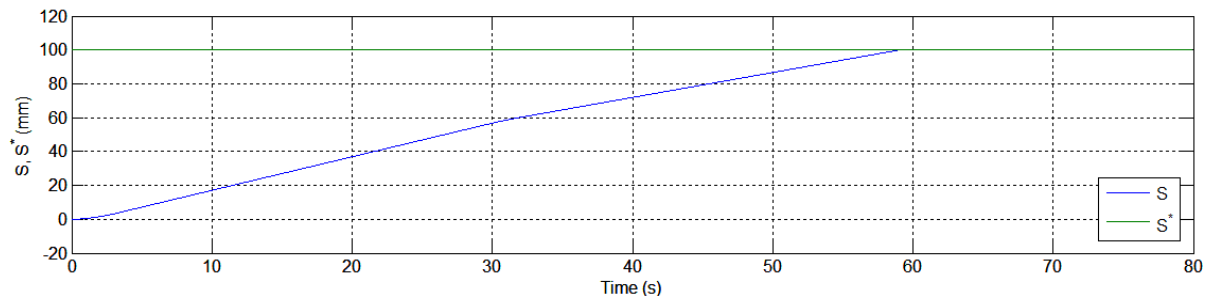

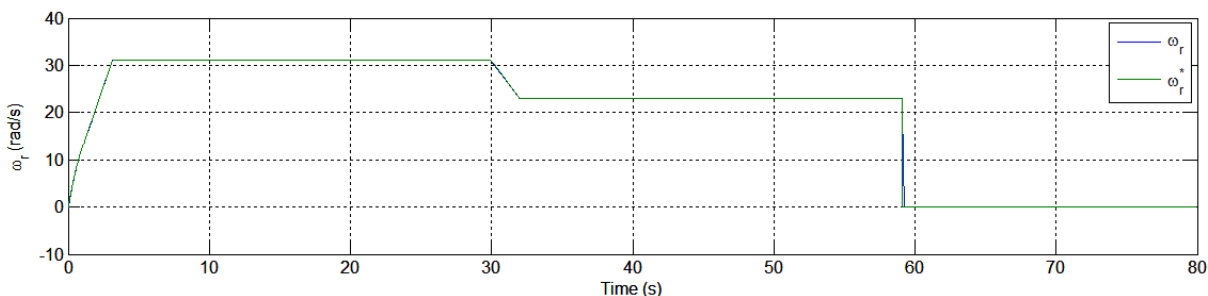Figure 8. Response and reference curves of the position of the X base.

Figure 9. Response and reference curves of rotational speed of the rotor.

In Figure 10, the response and reference curves of the X base speed are shown, in which the amplitude of 1.984 mm/s of the ramp reference was equivalent to the 31 rad/s amplitude, and amplitude of 1.472 mm/s was equivalent to the amplitude of 23 rad/s. By analyzing the graphics of Fig. 9 and 10, null steady state errors were observed in the time interval in which speed references were constant.
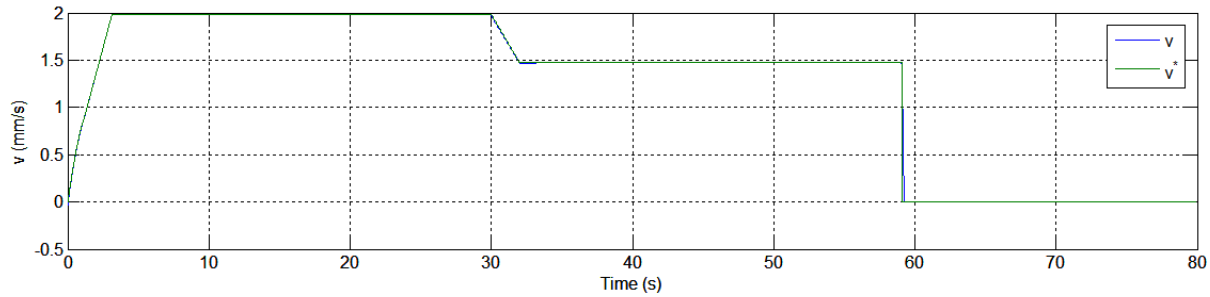
Figure 10. Response and reference curves of X base speed.

Following, the response and reference curves of the stator current in the d and q components were analyzed, as shown in Fig. 11 and 12, respectively. In these graphics, the control of both components of the stator current was verified. In Figure 12, it was possible to observe the behavior of the i_{sq}^{b*} control variable curve, generated by the fuzzy controller of speed, verifying the current increase from 30 s, moment from which the electromagnetic torque imposed on the three-phase induction motor was increased from 1 N.m to 3 N.m.
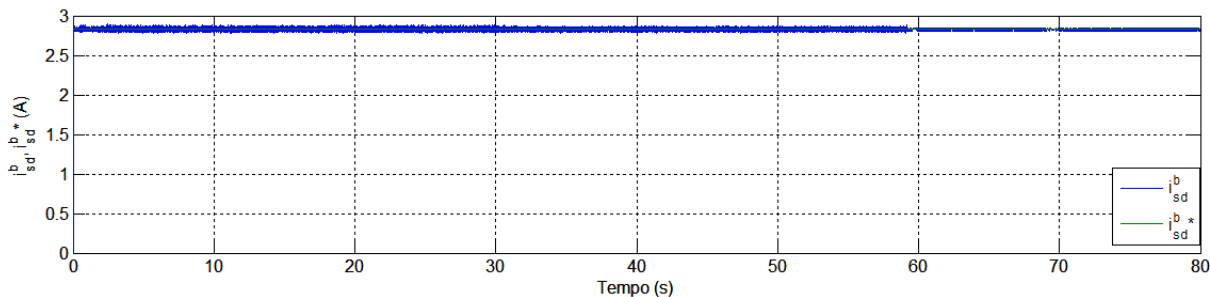
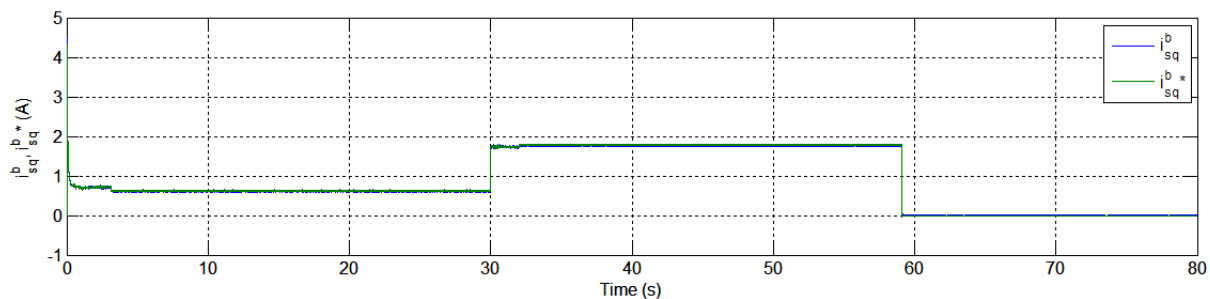Figure 11. Response and reference curves of the stator current in the d component.

Figure 12. Response and reference curves of the stator current in the q component.

For the analysis of neural estimation of the electromagnetic torque, in Figure 13, the ce electromagnetic torque curve obtained by modeling of the motor, using Eq. (10), and the ce_{est} estimated electromagnetic torque curve obtained by Eq. (16) were observed. In this graphic, the behavior of ce_{est} torque in the load transitory and in the steady state of estimation was verified. For applications of the first load, 1 N.m, and of the second load, 3 N.m, distinctions between ce and ce_{est} curves were rarely observed in the steady state.
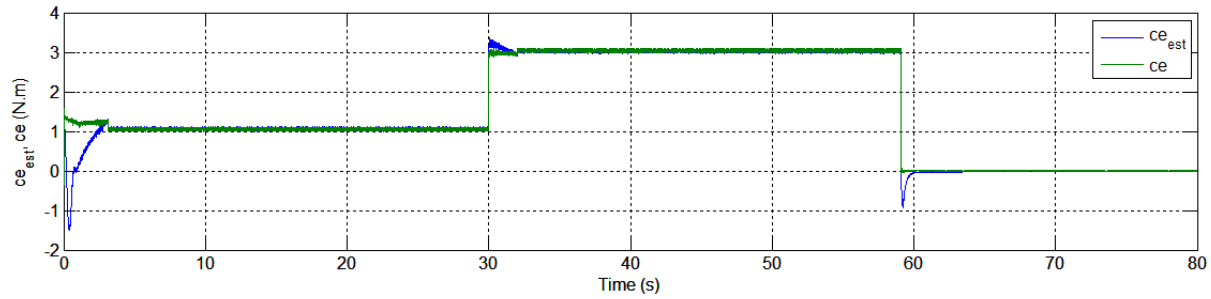
Figure 13. Curves of the electromagnetic torque and of the estimated electromagnetic torque.

3.2 Second simulation

In this simulation, firstly, a load of -2 N.m was applied, and, after 45 s of operation, a -5 N.m load was applied.

In Figure 14, the response and reference curves of angular position of the rotor are shown, for a motor drive by step reference signal with amplitude of -1562.5 rad. In Figure 15, the response curve and the step reference of the position of the X base with amplitude of -100 mm are presented. This amplitude in millimeters is equivalent to a step of -1562.5 rad, corresponding to a position of -100 mm in the X base. Through the graphics of Fig. 14 and 15, it was possible to verify a settling time of 67.65 s, a steady state error of 0.03 % and non-occurrence of overshoot.
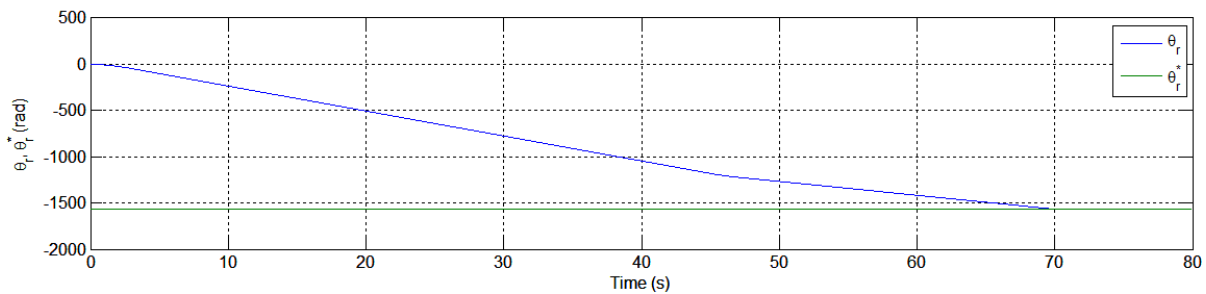

Figure 14. Response and reference curves of the angular position of the rotor.
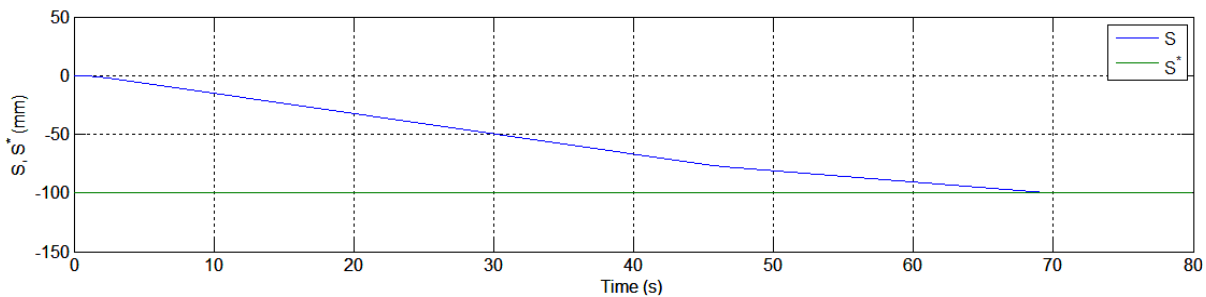

Figure 15. Response and reference curves of the position of the X base.

Then, in Fig. 16, the reference curve of the rotation speed of the rotor and the response curve obtained are shown. In this graphic, the excitation of the machine for speed ramp with amplitude of -27 rad/s was in the downward direction, keeping constant speed until the instant of 45 s. This constant speed of -27 rad/s corresponded to the ω_r^* reference due to an estimation of electromagnetic torque of -2 N.m. At the instant of 45 s, due to torque estimation of -5 N.m, a speed ramp with amplitude of -15 rad/s was used, in the upward direction, remaining constant up to a drive ω_r^* at null value.

In Figure 17, the response and reference curves of the X base speed are presented, in which the amplitude of -1.728 mm/s of the reference ramp is equivalent to the amplitude of -27 rad/s, and the amplitude of -0.96 mm/s is equivalent to the amplitude of -15 rad/s. Through the graphics of Fig. 16 and 17, null steady state errors were observed in the time interval in which speed references were constant.
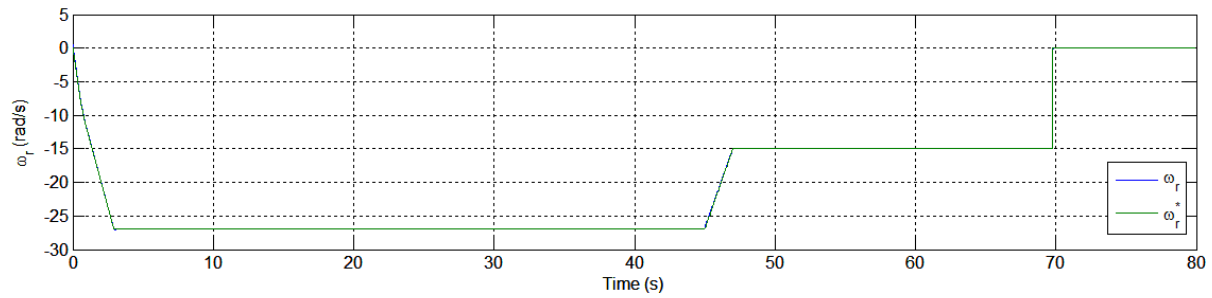
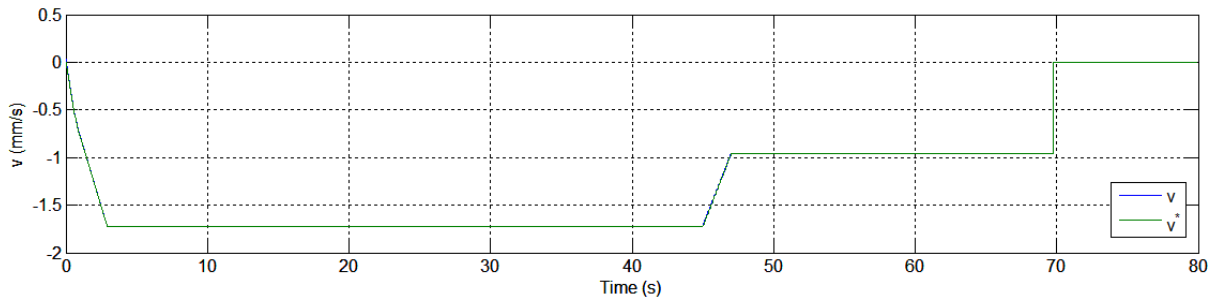Figure 16. Response and reference curves of rotational speed of the rotor.

Figure 17. Response and reference curves of the X base speed.

In Figures 18 and 19, the components of the stator current d and q are presented, respectively. In these graphics, it was verified that the components of the stator current were controlled. In Figure 19, from 45 s, the increase of the module of the currents i_{sq}^{b*} and i_{sq}^{b} was verified, because, from that instant, the module of the electromagnetic torque imposed on the motor was increased from -2 N.m to -5 N.m.

In Figure 20, the curves of the ce electromagnetic torque and of the ce_{est} estimated electromagnetic torque are shown. In this graphic, it was possible to verify the behavior of the ce_{est} torque in the load transitory and in the steady state of estimation. In the steady state, distinctions between ce and ce_{est} curves were rarely observed.
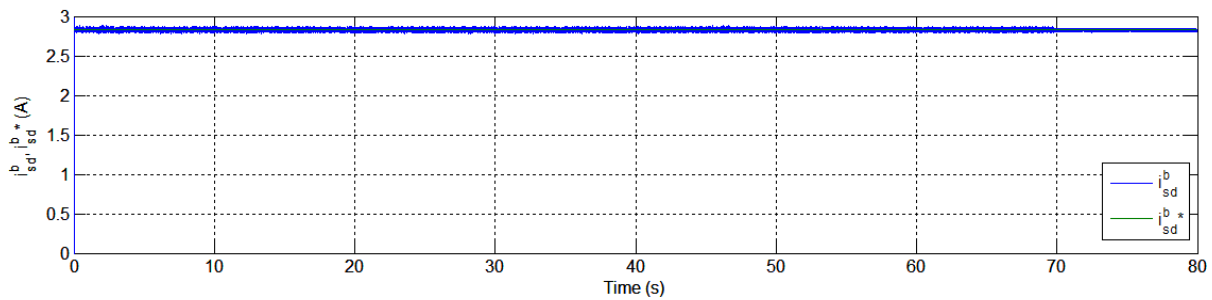
Figure 18. Response and reference curves of the stator current in the d component.
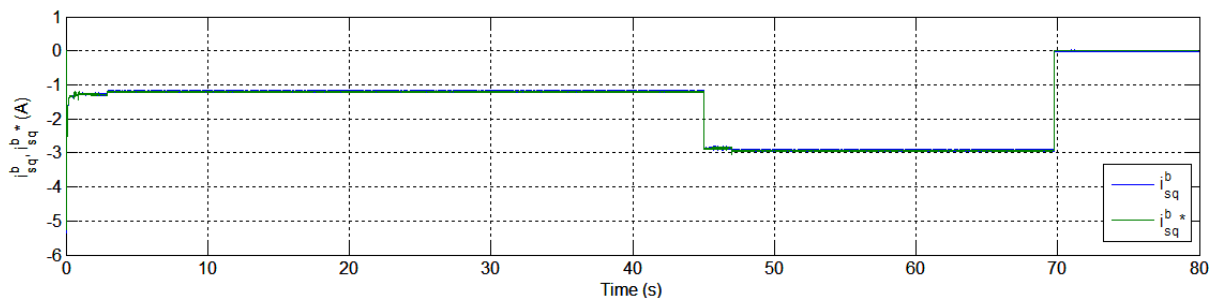
Figure 19. Response and reference curves of the stator current in the q component.
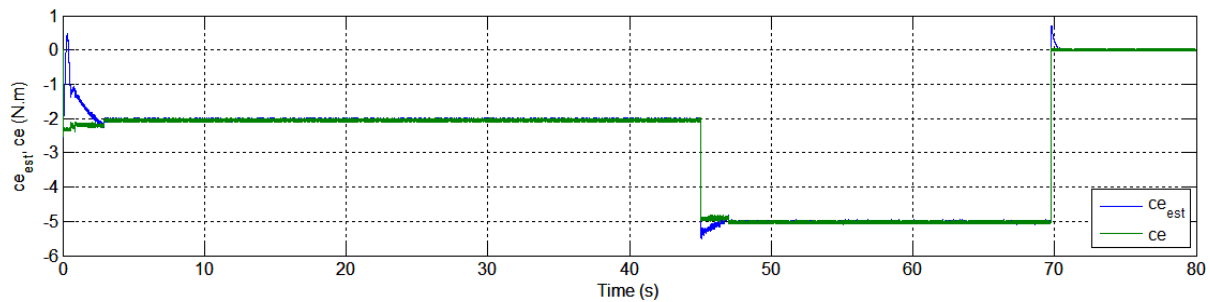
Figure 20. Curves of the electromagnetic torque and of the estimated electromagnetic torque.

4. COMMENTS AND CONCLUSIONS

In this work, the simulation of a control system for application in a milling system was presented. A three-phase induction motor was used, controlled by intelligent control techniques, to drive the milling machine table.

The performance of the control system was verified for the two directions of displacement of X base of the table, with changes in the electromagnetic torque imposed on the motor.

In analyzing the results, a criterion of 2 % of the amplitudes of the references was used. Through the response curves of the two simulations, a maximum steady state error of 0.13 % was verified for the variable position, not existing overshoot in any of the tests. For the speed, the fuzzy controller made possible the obtaining of null steady state errors in both simulations, at intervals drive with constant speeds. Regarding the electromagnetic torque, the convergence of the two signals of torque estimation was observed, obtaining small errors in comparing the curves of *ce* and of *ce*$_{est}$ in the steady state.

The fuzzy controller of speed, using the Takagi-Sugeno method, and the neural estimator of the electromagnetic torque, using the LMS algorithm technique, made possible the obtaining of satisfactory performance of the dynamic functioning of the motor.

An important contribution of this work is the specification of the rotational speed of the rotor of a three-phase induction motor from the information of the signal of the estimated electromagnetic torque, using intelligent control techniques.

As perspective of future work, it is planned to carry out experimental tests in a milling machine, with the feedrate specified in real time from the machining of each material.

5. REFERENCES

Altuna, J.A.T., 1997. *Implementação do método direto do controle vetorial de um motor de indução, com orientação de fluxo do estator utilizando DSP*. Dissertação de M.Sc., Universidade Estadual de Campinas, Campinas, SP, Brasil.

Alves, C.A.F.C., 2002. *Estudo da nitretação a plasma aplicada em ferramentas para fresamento*. Dissertação de M.Sc., Universidade Federal do Rio Grande do Sul, Porto Alegre, RS, Brasil.

Leite, L.C., 2003. *Identificação do conjugado de uma máquina de indução setorial via redes neurais artificiais*. Tese de D.Sc., Universidade Estadual de Campinas, Campinas, SP, Brasil.

Lin, X., Li, A. and Zhang, W., 2006. "Learning fuzzy logic based intelligent determination of feedrate for end milling operation". *IEEE Computer Society*, In *6th International Conference on Intelligent Systems Design and Applications (ISDA'06)*.

Mao-Yue, L., Hong-Ya, F., Yuan, L. and Zhen-Yu, H., 2009. "An intelligent controller based on constant cutting force for 5-axis milling". *IEEE Computer Society*, In *International Conference on Information Technology and Computer Science*, p. 237-241.

Milhor, C.E., 2008. *Proposta de um controlador difuso Takagi-Sugeno com desempenho H_∞ para regulagem da marcha lenta em motores de ciclo otto*. Tese de D.Sc., Escola de Engenharia de São Carlos, Universidade de São Paulo, São Carlos, SP, Brasil.

Mozelli, L.A., 2008. *Controle fuzzy para sistemas Takagi-Sugeno: condições aprimoradas e aplicações*. Dissertação de M.Sc., Universidade Federal de Minas Gerias, Belo Horizonte, MG, Brasil.

Nigrini, A., 1993. *Neural Networks for Pattern Recognition*. The MIT Press, Cambridge.

Rumelhart, D.E. and Mcclelland, J.L., 1986. *Parallel Distributed Processing: Explorations in the Microstructure of Cognition*. The MIT Press, PDP Research Group, University of California, San Diego.

Severino, P.B., 2005. *Um estudo de estimativa de fluxo e conjugado em motores de indução trifásicos – implementação utilizando DSP*. Dissertação de M.Sc., Universidade Federal de Uberlândia, Uberlândia, MG, Brasil.

Shaw, I.S. and Simões, M.G., 2004. *Controle e Modelagem Fuzzy*. Editora Edgard Blucher Ltda, São Paulo, SP, Brasil.

Takagi, T. and Sugeno, M., 1985. "Fuzzy identification of systems and its application to modelling and control". *IEEE Transactions on Systems, Man and Cybernetics*, Vol. SMC-15, n. 1, p. 116-132.

6. RESPONSIBILITY NOTICE

The authors are the only responsible for the printed material included in this paper.